

PAPER • OPEN ACCESS

## High harmonic generation- $2\omega$ attosecond stereo-photoionization interferometry in $N_2$

To cite this article: V Lorient *et al* 2020 *J. Phys. Photonics* 2 024003

View the [article online](#) for updates and enhancements.

### Recent citations

- [Attosecond spectroscopy of liquid water](#)  
Inga Jordan *et al*
- [Glory oscillations in photoionization microscopy: Connection with electron dynamics and Stark spectral structures in the continuum](#)  
P. Kalaitzis *et al*



## PAPER

## OPEN ACCESS

High harmonic generation- $2\omega$  attosecond stereo-photoionization interferometry in  $N_2$ RECEIVED  
16 December 2019REVISED  
5 February 2020ACCEPTED FOR PUBLICATION  
28 February 2020PUBLISHED  
31 March 2020V Lorient<sup>1</sup> , A Marciniak<sup>1</sup> , S Nandi<sup>1</sup> , G Karras<sup>1</sup> , M Hervé<sup>1</sup> , E Constant<sup>1</sup> , E Plésiat<sup>2</sup>,  
A Palacios<sup>2</sup> , F Martín<sup>2,3,4</sup> and F Lépine<sup>1</sup> <sup>1</sup> Univ Lyon, Univ Claude Bernard Lyon 1, CNRS, Institut Lumière Matière, F-69622, Villeurbanne, France<sup>2</sup> Departamento de Química, Módulo 13, Universidad Autónoma de Madrid, 28049 Madrid, Spain<sup>3</sup> Instituto Madrileño de Estudios Avanzados en Nanociencia (IMDEA-Nanociencia), Cantoblanco, 28049 Madrid, Spain<sup>4</sup> Condensed Matter Physics Center (IFIMAC), Universidad Autónoma de Madrid, 28049 Madrid, SpainE-mail: [vincent.lorient@univ-lyon1.fr](mailto:vincent.lorient@univ-lyon1.fr)

Original Content from this work may be used under the terms of the [Creative Commons Attribution 4.0 licence](https://creativecommons.org/licenses/by/4.0/). Any further distribution of this work must maintain attribution to the author(s) and the title of the work, journal citation and DOI.

**Keywords:** photoionization, attosecond, electron diffusion, ionization delays, molecular ionization**Abstract**

We have investigated photoionization delays in  $N_2$  by combining an extreme ultraviolet (XUV) attosecond pulse train generated by high harmonic generation (HHG) and a second harmonic femtosecond pulse with angularly resolved photoelectron spectroscopy. While photoionization delay measurements are usually performed by using a standard XUV-infrared scheme, here we show that the present approach allows us to separate electronic states that otherwise would overlap, thus avoiding the spectral congestion found in most molecules. We have found a relative delay between the  $X$  and  $A$  ionic molecular states as a function of the photon energy of up to 40 attoseconds, which is due to the presence of a shape resonance in the  $X$  channel. This approach can be applied to other small quantum systems with few active electronic states.

**1. Introduction**

Photoionization has been used as a tool for investigating quantum effects in atoms and molecules. In that context, extreme ultraviolet (XUV) radiation delivered by synchrotron light sources has permitted to explore the richness of ionization continua, revealing resonances and their nature [1]. The electron dynamics associated to these spectral features span over a broad range of timescales, which can reach the attosecond domain for broad resonances. Such dynamics remained inaccessible until the recent development of attosecond physics and high-order harmonic generation (HHG) based sources providing ultrashort XUV pulses. In atoms, it has led to progresses in the understanding of electron wavepacket dynamics [2], resonance reconstruction [3], and attosecond coherent imaging [4]. Among the techniques developed, the so-called 'delay in photoemission' measurements [5] have been able to address new features in photoionization processes. In such experiments, a typical protocol is to use a two-color scheme that combines an XUV and a delayed fundamental near infrared (NIR) pulse. Following ionization by the XUV pulse, the emitted electron wavepacket acquires a phase due to its scattering in the potential of the residual ion. Based on the concept proposed by Wigner, the derivative of this phase with respect to the electron kinetic energy corresponds to the semi-classical scattering time delay [6]. Considering photoionization as a half-scattering process, this can be regarded as photoionization delay. The scattering phase, and hence the photoionization delay, can be extracted from the measured XUV-NIR delay dependent photoelectron spectrum. Attosecond photoionization time delays have been investigated in atoms, to measure variations of emission time between electrons coming from different orbitals [5, 7–9] as well as delays induced by resonances [10], eventually leading to the possibility to reconstruct the building-up dynamics of a Fano profile [3].

Compared to atoms, molecules provide a richer electronic structure, a breaking of spherical symmetry and additional nuclear degrees of freedom. It challenges not only the concept of Wigner delay, but also raises the question of the specificity of molecular photoionization mechanisms [11–17]. The RABBIT (Reconstruction of Attosecond Beating By Interference of Two-photon transitions) method [18] has been successfully used in attosecond photoemission time delay measurements as it combines both spectral and

temporal resolution [9] by using an attosecond pulse train (APT) composed of a harmonic frequency comb. It has been extensively used for atomic targets and was first applied to molecules in a seminal work performed on nitrogen [19, 20]. In that work, low order harmonics were used to study phase variations due to Hopfield resonance, with vibrational resolution. More recently, other authors have reported the first investigation of triatomic molecules for which the effect of a shape resonance were described in  $N_2O$ , leading to a time delay of 160 as between the two outermost orbitals while a few attoseconds delay were observed in  $H_2O$  in absence of the resonance [16, 17]. Approaches combining RABBIT and coincidence measurements also allowed to investigate orientation dependent time delays [21, 22], opening new avenues in this context. One of the advantages of the RABBIT technique is that the interference pattern arises from only 2 quantum paths. As a consequence, it carries information that only depends on the relative phases of the corresponding transitions. Nevertheless, the generalisation of the photoemission delay measurements in molecules faces an intrinsic limitation: the RABBIT method inevitably leads to a congested electron spectrum formed by the superposition of bands and sidebands due to the many electronic states and to the APT frequency comb. This is seen as an important issue of the RABBIT method to explore complex molecular systems [16, 23].

In the current work, we investigate photoionization delays the nitrogen molecule where two active electronic states are separated by less than 1.5 eV. It is known that in a standard RABBIT scheme, the contribution of these states partially overlap [19] restraining the accessible information. Here, we investigate the possibility to experimentally separate the two electronics states by employing the second harmonic instead of the fundamental field. Combined with angularly resolved electron spectrometry, we show that it allows to study variation of photoionization time delays with attosecond timescale resolution while avoiding the spectral congestion. We observe variations of the phase in the  $X$ -state that is attributed to the presence of the shape resonance. Our results are in agreement with theoretical calculations based on single photon ionization [24–26].

## 2. Method

In our experiment, we use a chirped pulse amplified laser system (CEP-stable Legend elite USX by Coherent) with spectrum centered at  $\sim 800$ nm,  $\sim 20$  femtoseconds output pulse duration, 2 mJ energy per pulse, and 5 kHz repetition rate. The output is split into two parts with one being used to create an APT through the HHG process in Xenon gas. The APT in the spectral domain is an XUV frequency comb of equidistant odd-order harmonics of the fundamental NIR, which is filtered out after passing through a 200 nm thick Aluminum filter. A typical spectrum of the XUV frequencies used in the experiment spanned from 17 eV up to 33 eV (from HH11 to HH21). The XUV field is focused inside the interaction region of a velocity map imaging spectrometer (VMIS) [27] where the nitrogen is introduced as an effusive jet through a small hole in the repeller electrode. The remaining part of the fundamental beam is frequency doubled using a 500  $\mu$ m thick  $\beta$ -Barium Borate (BBO) crystal, leading to a 7 nm (45 meV) bandwidth pulse at 400 nm. The remaining 800 nm beam is filtered out using a dichroic mirror. The 400 nm pulse is focused inside the VMIS and spatio-temporally overlapped with the APT.

Electrons with the same final kinetic energy can be created from three excitation pathways, due to single photon (XUV) or two-photon (XUV  $\pm$  400 nm) transitions [28, 29]

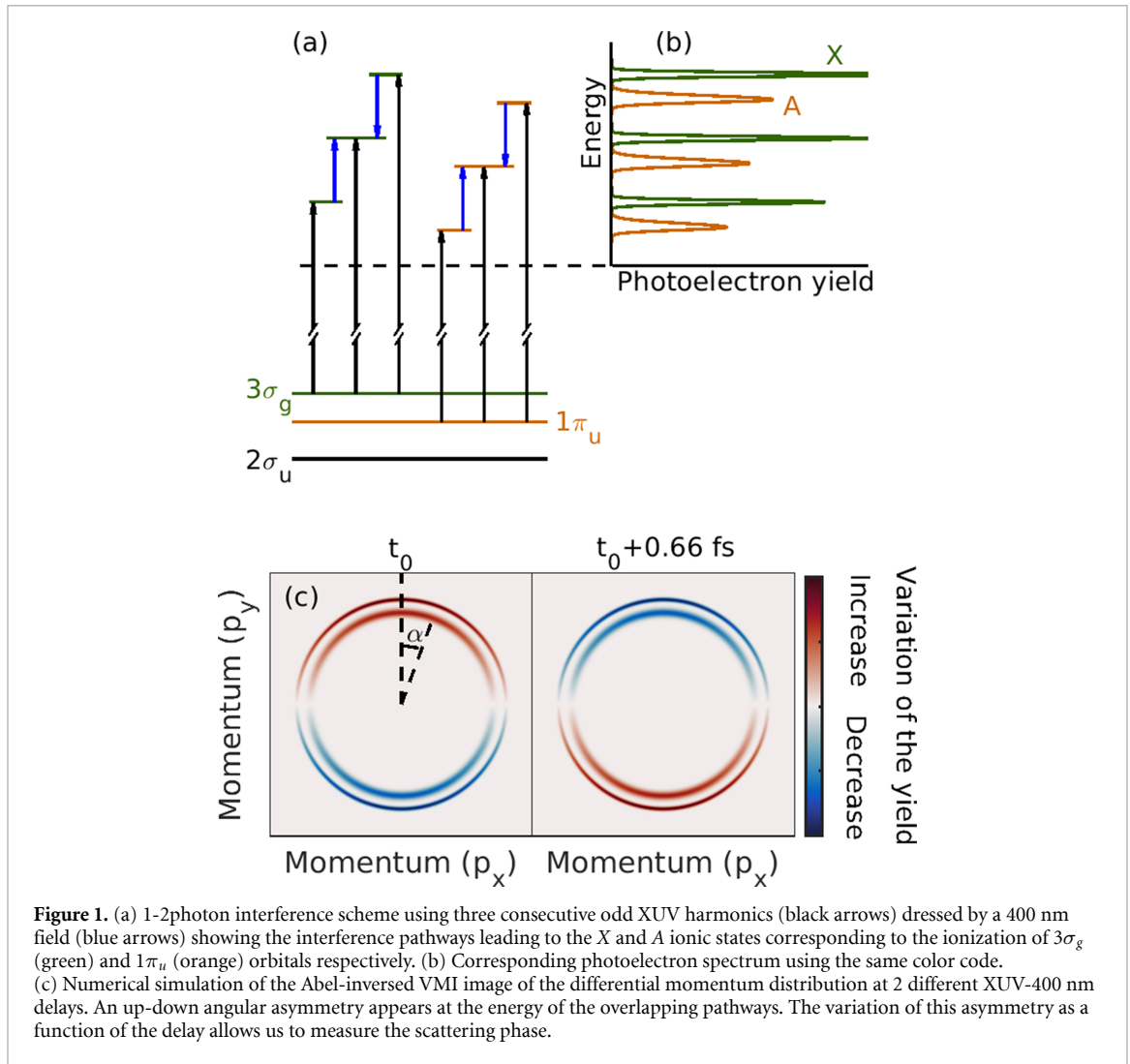
$$E_n^i = n \times \hbar\omega_0 - IP_i, \quad (1)$$

$$E_{n-}^i = (n-2) \times \hbar\omega_0 + 2\hbar\omega_0 - IP_i, \quad (2)$$

$$E_{n+}^i = (n+2) \times \hbar\omega_0 - 2\hbar\omega_0 - IP_i, \quad (3)$$

with  $\omega_0$  the frequency of the fundamental NIR pulse and  $IP_i$  the ionization potential of the electronic state  $i$ . Equation (1) involves the absorption of one XUV photon from the harmonic  $n$ , while the equations (2) and (3) involve the absorption of one XUV photon from the harmonic ( $n \mp 2$ ) with the absorption or the emission of a 400 nm photon respectively (see figure 1(a)).

The one and two-photon pathways lead to an interference between wavefunctions of different parity. In an atomic case, this would correspond to an interference between  $l$  and  $(l \pm 1)$  partial waves, producing an up-down, delay dependent asymmetry of the photoelectron angular distribution with respect to the light polarization. More generally, decomposing the angularly resolved photoelectron spectrum as a sum of even and odd Legendre polynomials shows that the recorded signal has an up-down asymmetry with respect to the polarization axis (see figure 1(c)). In the following, the electron signal ( $S_{up}$ ) is integrated over emission



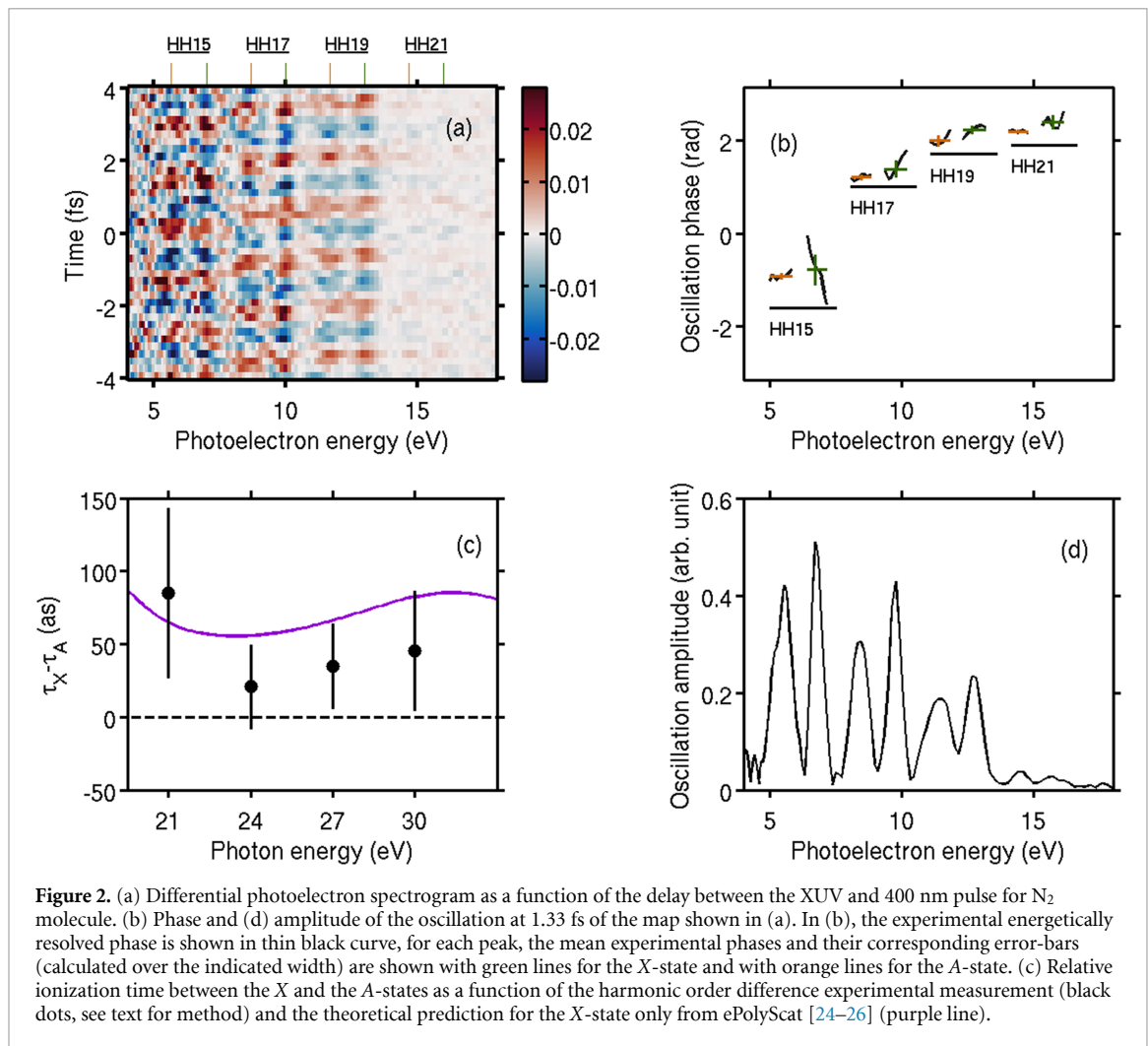
**Figure 1.** (a) 1-2-photon interference scheme using three consecutive odd XUV harmonics (black arrows) dressed by a 400 nm field (blue arrows) showing the interference pathways leading to the X and A ionic states corresponding to the ionization of  $3\sigma_g$  (green) and  $1\pi_u$  (orange) orbitals respectively. (b) Corresponding photoelectron spectrum using the same color code. (c) Numerical simulation of the Abel-inversed VMI image of the differential momentum distribution at 2 different XUV-400 nm delays. An up-down angular asymmetry appears at the energy of the overlapping pathways. The variation of this asymmetry as a function of the delay allows us to measure the scattering phase.

angles on the upper part of the image ( $\pm\pi/2$  around the polarization axis). An integration over the lower part of the image would lead to the opposite signal that corresponds to a global  $\pi$ -shift on the phase measurement ( $S_{\text{down}} = -S_{\text{up}} = S_{\text{up}}e^{i\pi}$ ). The term oscillating at  $2\omega_0$  (1.33 fs) can be described by perturbation theory as shown in Laurent *et al* [28]

$$S_n^i(t) = A_n \left[ A_{n-2} \cos(2\omega_0 t + \varphi_{n-2} - \varphi_n) - A_{n+2} \cos(2\omega_0 t + \varphi_n - \varphi_{n+2}) \right], \quad (4)$$

with  $t$  being the delay between the XUV and 400 nm pulses.  $A_n$  denotes the amplitude of the contribution at the harmonic order  $n$ ,  $\varphi_n$  the total phase (the sum of the harmonic phase  $\varphi_n^{HH}$ , the phase acquired by the escaping electron wavepacket  $\varphi_n^{mol}$ , and the continuum-continuum phase  $\varphi_n^{cc}$ ) at the harmonic order  $n$ . Since all contributions are oscillating at  $2\omega_0$ , the resulting global oscillation also oscillates at 1.33 fs. Hence, the amplitude and the phase of this global oscillation depends on the amplitude and the phase of the harmonic order  $(n-2)$ ,  $n$ , and  $(n+2)$ . This is in contrast with the RABBIT method, where the resulting oscillation phase arises from the interference of only two contributions and the final oscillation phase does not depend on the amplitudes.

From figure 1(a), it can also be noticed that a standard RABBIT scheme can take place at higher intensities of the dressing field invoking a higher order of perturbation theory term involving  $(2+2)$  photons (instead of  $(2+1)$ ). The interfering paths consider the harmonics  $A_{n-2}$  and  $A_{n+2}$  dressed by the  $2\omega_0$  field leading to a sideband overlapped with the contribution at  $A_n$ . However, this scheme would lead to an oscillation at  $4\omega_0$  (665 as) and would not present an up/down asymmetry. We checked in our measurements that no oscillations at four times the NIR frequency are measured, and the even order of asymmetry does not evolve.



### 3. Ionization to the X state of nitrogen

Figure 2(a) shows the experimental differential spectrogram obtained by angularly integrating the signal over the top side of the image and subtracting the signal obtained with XUV alone. For each harmonic, two contributions appear corresponding to two ionic states X ( $^2\Sigma_g^+$ ) and A ( $^2\Pi_u$ ) with vertical ionization potentials of  $IP_X = 15.60$  eV and  $IP_A = 16.98$  eV respectively [30]. For each electron kinetic energy, the signal may have contributions from all the aforementioned processes (1), (2) and (3). For example, electrons with kinetic energy of 12.7 eV could originate either from one photon (HH19) and/or two-photon (HH17+ $2\omega_0$  or HH21- $2\omega_0$ ) absorption processes. By varying the time delay,  $t$ , between the 400 nm and the XUV pulses, interference between the different ionization pathways occur, leading to an oscillation with a periodicity of 1.33 fs.

Performing a Fourier transformation of the spectrogram on the time axis provides the phases and the amplitudes of the oscillations at 1.33 fs for each photoelectron energy as shown in figures 2(b) and (d). The use of  $2\omega_0$  (3.1 eV) as a dressing field allows us to disentangle the A and X ionic states separated by about 1.4 eV, which otherwise would overlap in a standard NIR ( $\sim 1.5$  eV) RABBIT. The phase of the A-state increases between HH17 and HH21 principally due to the so-called attochirp. This information can be used to reconstruct the temporal profile of the XUV attosecond pulse train [31]. Figure 2(b) show differences in the phase between the A and X ionic states as a function of the harmonic order. This difference clearly varies between 0.2 to 0.35 rad as a function of the harmonic order. In contrast to the RABBIT method, both the spectral phase and amplitude have to be reconstructed using equation (4). This is performed following a procedure similar to Laurent *et al* [29]. It allows us to reconstruct the phases  $\varphi_n(X)$  and  $\varphi_n(A)$ . The reconstruction of the X-state ionization time requires the following assumptions: (i) the continuum-continuum contribution on the phase ( $\varphi_n^{cc}(X) - \varphi_n^{cc}(A)$ ) can be neglected because of the small energy difference between the states (around few attoseconds following Dahlström *et al* [8]) (ii)  $\varphi_n^{mol}(A) \approx 0$  since the A-state does not present any resonance in this spectral region [25] (only few attoseconds shift are

expected) (iii)  $\varphi_n^{HH}(A) = \varphi_n^{HH}(X)$  because they are measured with the same harmonic spectrum. Consequently, the phase difference allows us to extract the ionization time [6] of the  $X$ -state ( $\tau_X = (\varphi_{n+1}(X) - \varphi_{n-1}(X))/2\hbar\omega_0$ ) with respect to the  $A$ -state ( $\tau_A = (\varphi_{n+1}(A) - \varphi_{n-1}(A))/2\hbar\omega_0$ ), as shown in figure 2(c).

This experimental result can be compared with the one-photon matrix element calculation performed by Hockett *et al* [24, 32] from ePolyScat suite codes [25, 26, 33]. In this calculation, the transition matrix elements of the  $X$ -state is calculated at the first order perturbation theory, for different polarization and using dipole and fixed nuclei approximations. Since the gaseous nitrogen sample is randomly oriented, the ionization time has been averaged over the molecular orientations following the method given by Baykusheva and Wörner [16].

The result of the calculation is presented in figure 2(c) and compared to the experimental results. A reasonably good agreement between the experimental and theoretical results is found. Comparing theory and experiment, the phase of the  $X$ -state remains positive (above the one of the  $A$ -state) across the studied photon energy range. A drop in the ionization time is observed around 24 eV, with a phase increase up to  $\sim 30$  eV. From the calculation, this variation is attributed to the presence of a shape resonance in the  $X$ -state [24]. Such resonance in the  $X$  ionic-channel has already been identified in synchrotron experiments, while the  $A$  ionic-state is known to exhibit no structure in the continuum [25]. In other words, the variation of the phase between  $X$  and  $A$ -states should principally reflect the phase variation of the  $X$ -state, namely the shape resonance effect. This justifies the qualitative agreement with our calculations that contains only the  $X$  channel.

Classically, a shape resonance is a signature of an excited electron that is trapped in a quasi-bound state by the molecular potential. Eventually, the electron can tunnel through the potential and escape to the continuum. When the phase variation is converted into time delay following the Wigner formalism [6], the measured phase variation corresponds to a positive time delay. This agrees with the intuitive classical picture of electron dynamics being determined by the shape of the molecular potential. The delay varies between 45 to 65 attoseconds across the resonance. In the spectral domain, since the width of the resonance [34] is around 8 eV, this would correspond to a lifetime of  $\sim 80$  as. The direct link between photoemission delay and spectral width has already been discussed, for instance in the case of autoionizing resonances [35]. Although this link cannot be generalized, our time-resolved measurements give a reasonably good agreement with the lifetime close to the resonance maximum (at HH21). It also provides a direct information of how this lifetime varies as a function of the detuning with respect to the maximum of the resonance [36]. Indeed, the measurement of the ionization time delay carries information on the quantum phase involved in the dipolar transition, which provides a more accurate description of the structure of the continuum compared to spectrally resolved yield measurements.

## 4. Conclusion

We propose a HHG- $2\omega$  attosecond interferometric scheme combined with angularly resolved photoelectron spectroscopy to perform attosecond photoionization delay measurements. Although, this approach requires a more complex reconstruction procedure to extract the phase information, our approach allows to separate electronic states that otherwise overlap when using a standard RABBIT with a 800 nm dressing field. This method is applied to  $N_2$  in a spectral region of structured continuum. Variation of the phase is measured and is attributed to the presence of a shape resonance in the  $X$ -state, in agreement with single photon ionization calculations. This shows that the present method allows to investigate molecular effects down to attosecond timescale resolution without further congestion of the photoelectron spectrum.


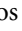


## Acknowledgments

We acknowledge A L'Huillier, M Gisselbrecht and H J Wörner for fruitful discussions. We acknowledge the support of CNRS, ANR-16-CE30-0012 'Circé', ANR-15-CE30-0001 'CIMBAAD' and the Fédération de recherche André Marie Ampère. EP, AP and FM are supported by the MINECO grant FIS2016-77889-R. FM acknowledges support from the 'Severo Ochoa' Programme for Centres of Excellence in R&D (MINECO, Grant SEV-2016-0686) and the 'Maria de Maeztu' Programme for Units of Excellence in R&D (MDM-2014-0377).

## ORCID iDs

V Lorient  <https://orcid.org/0000-0002-5986-6664>

A Marciniak  <https://orcid.org/0000-0002-1703-0041>

S Nandi  <https://orcid.org/0000-0002-8776-8092>  
G Karras  <https://orcid.org/0000-0002-9629-8336>  
M Hervé  <https://orcid.org/0000-0003-2291-6469>  
E Constant  <https://orcid.org/0000-0002-3304-6860>  
A Palacios  <https://orcid.org/0000-0001-6531-9926>  
F Martín  <https://orcid.org/0000-0002-7529-925X>  
F Lépine  <https://orcid.org/0000-0001-9040-919X>

## References

- [1] Becker U and Shirley D A 1996 *VUV and Soft X-Ray Photoionization* (New York: Plenum Press)
- [2] Remetter T et al 2006 Attosecond electron wave packet interferometry *Nat. Phys.* **2** 323
- [3] Gruson V et al 2016 Attosecond dynamics through a fano resonance: Monitoring the birth of a photoelectron *Science* **354** 734–8
- [4] Villeneuve D M, Hockett P, Vrakking M J J and Niikura H 2017 Coherent imaging of an attosecond electron wave packet *Science* **356** 1150–3
- [5] Schultze M et al 2010 Delay in photoemission *Science* **328** 1658–62
- [6] Wigner E P 1955 Lower limit for the energy derivative of the scattering phase shift *Phys. Rev.* **98** 145–7
- [7] Klünder K et al 2011 Probing single-photon ionization on the attosecond time scale *Phys. Rev. Lett.* **106** 143002
- [8] Dahlström J M, Guénot D, Klünder K, Gisselbrecht M, Mauritsson J, L'Huillier A, Maquet A and Taïeb R 2013 Theory of attosecond delays in laser-assisted photoionization *Chem. Phys.* **414** 53–64 Attosecond spectroscopy
- [9] Isinger M et al 2017 Photoionization in the time and frequency domain *Science* **358** 893–6
- [10] Cirelli C et al 2018 Anisotropic photoemission time delays close to a fano resonance *Nat. Commun.* **9** 955
- [11] Lépine F, Ivanov M Y and Vrakking M J J 2014 Attosecond molecular dynamics: fact or fiction? *Nat. Photon.* **8** 195
- [12] Vrakking M J J and Lépine F 2019 *Attosecond Molecular Dynamics* Theoretical and Computational Chemistry Series (London: The Royal Society of Chemistry)
- [13] Lara-Astiaso M et al 2018 Attosecond pump-probe spectroscopy of charge dynamics in tryptophan *J. Phys. Chem. Lett.* **9** 4570–7 PMID30044916
- [14] Drescher L, Reitsma G, Witting T, Patchkovskii S, Mikosch J and Vrakking M J J 2019 State-resolved probing of attosecond timescale molecular dipoles *J. Phys. Chem. Lett.* **10** 265–9
- [15] Despré V, Marciniak A, Lorient V, Galbraith M C E, Rouzée A, Vrakking M J J, Lépine F and Kuleff A I 2015 Attosecond hole migration in benzene molecules surviving nuclear motion *J. Phys. Chem. Lett.* **6** 426–31
- [16] Baykusheva D and Wörner H J 2017 Theory of attosecond delays in molecular photoionization *J. Chem. Phys.* **146** 124306
- [17] Huppert M, Jordan I, Baykusheva D, von Conta A and Wörner H J 2016 Attosecond delays in molecular photoionization *Phys. Rev. Lett.* **117** 093001
- [18] Paul P M, Toma E S, Breger P, Mullot G, Augé F, Balcou P, Muller H G and Agostini P 2001 Observation of a train of attosecond pulses from high harmonic generation *Science* **292** 1689–92
- [19] Haessler S et al 2009 Phase-resolved attosecond near-threshold photoionization of molecular nitrogen *Phys. Rev. A* **80** 011404
- [20] Caillat Jémie, Maquet A, Haessler S, Fabre B, Ruchon T, Salières P, Mairesse Y and Richard Tieb 2011 Attosecond resolved electron release in two-color near-threshold photoionization of N<sub>2</sub> *Phys. Rev. Lett.* **106** 093002
- [21] Vos J, Cattaneo L, Patchkovskii S, Zimmermann T, Cirelli C, Lucchini M, Kheifets A, Landsman A S and Keller U 2018 Orientation-dependent stereo wigner time delay and electron localization in a small molecule *Science* **360** 1326–30
- [22] Cattaneo L et al 2018 Attosecond coupled electron and nuclear dynamics in dissociative ionization of H<sub>2</sub> *Nat. Phys.* **14** 733
- [23] Jordan I and Wörner H J 2018 Extracting attosecond delays from spectrally overlapping interferograms *J. Opt.* **20** 024013
- [24] Hockett P, Frumker E, Villeneuve D M and Corkum P B 2016 Time delay in molecular photoionization *J. Phys. B: At. Mol. Opt. Phys.* **49** 095602
- [25] Lucchese R R, Raseev G and Vincent M 1982 Studies of differential and total photoionization cross sections of molecular nitrogen *Phys. Rev. A* **25** 2572–87
- [26] Lucchese R R ([www.chem.tamu.edu/rgroup/lucchese/](http://www.chem.tamu.edu/rgroup/lucchese/))
- [27] André T J B E and Parker D H 1997 Velocity map imaging of ions and electrons using electrostatic lenses: Application in photoelectron and photofragment ion imaging of molecular oxygen *Rev. Sci. Instrum.* **68** 3477–84
- [28] Laurent G, Cao W, Li H, Wang Z, Ben-Itzhak I and Cocke C L 2012 Attosecond control of orbital parity mix interferences and the relative phase of even and odd harmonics in an attosecond pulse train *Phys. Rev. Lett.* **109** 083001
- [29] Laurent G, Cao W, Ben-Itzhak I and Cocke C L 2013 Attosecond pulse characterization *Opt. Express* **21** 16914–27
- [30] Kimura K, Katsumata S, Achiba Y, Yamazaki T and Iwata S 1981 *Handbook of HeI Photoelectron Spectra of Fundamental Organic Molecules* (Tokyo: Japan Scientific Societies Press)
- [31] Lorient V et al 2017 Angularly resolved RABBITT using a second harmonic pulse *J. Opt.* **19** 114003
- [32] Hockett P, Frumker E, Villeneuve D M and Corkum P B 2016 *J. Phys. B* **49** 095602
- [33] Lucchese R R, Takatsuka K and McKoy V 1986 Applications of the schwinger variational principle to electron-molecule collisions and molecular photoionization *Phys. Rep.* **131** 147–221
- [34] West J B, Parr A C, Cole B E, Ederer D L, Stockbauer R and Dehmer J L 1980 Shape-resonance-induced non-franck-condon vibrational intensities in  $3\sigma_g$  photoionisation of N<sub>2</sub> *J. Phys. B: At. Mol. Phys.* **13** L105–L108
- [35] Dolmatov V K, Kheifets A S, Deshmukh P C and Manson S T 2015 Attosecond time delay in the photoionization of Mn in the region of the  $3p \rightarrow 3d$  giant resonance *Phys. Rev. A* **91** 053415
- [36] Kotur M et al 2016 Spectral phase measurement of a fano resonance using tunable attosecond pulses *Nat. Commun.* **7** 10566